No evidence of the 17-keV neutrino in the decay of ^{71}Ge

D. E. DiGregorio, S. Gil, H. Huck, E. R. Batista, A. M. J. Ferrero, and A. O. Gattone
Departamento de Física, TANDAR, Comisión Nacional de Energía Atómica, Avenida del Libertador 8250, 1429 Buenos Aires, Argentina
(Received 7 October 1992)

We have measured the internal bremsstrahlung spectrum of the electron capture decay of ^{71}Ge in search for a possible mass component of the emitted neutrino. The main relevance of this experiment is given by the collected statistics which is 20 times larger than in a previously published work studying the same decay. Analyses of the data exclude the presence of a massive component of $17.2^{+1.3}_{-1.1}$ keV and $(1.6 \pm 0.7)\%$ mixing fraction claimed by Zlimen *et al.* for this same nucleus, at the 99.0% confidence level.

PACS number(s): 23.40.Bw, 14.60.Gh, 27.50.+e

I. INTRODUCTION

The quest for the existence of a 17-keV neutrino first observed in nuclear weak transitions has been the origin of some recent intense activity on both the experimental as well as the theoretical side [1]. Until very recently, experiments had produced as many positive [2–7] as negative results [8–13], with most of the positive announcements reported in the past two years or so—with the exception of the pioneer work by Simpson [14] published in 1985. The renewed experimental efforts started to give new results that have been just (or are being) published, claiming that there is now convincing evidence against the existence of the heavy neutrino [15, 16]. Hime has just reanalyzed the Oxford data [17]—taking into account electron scattering effects—and found that these artifacts in the electron response function were sufficient to remove the observed anomalies claimed earlier as evidence for a 17-keV neutrino [3, 4]. All these just reported new experiments detected electrons generated in the nuclear β decay. The other weak-interaction decay in which a heavy neutrino might manifest is the inner bremsstrahlung accompanying the electron capture by a proton in the nucleus (IBEC). The IBEC experiments have produced results which are not in agreement with each other. Thus, while Norman *et al.* [2] first claimed to observe a neutrino mass component of (21 ± 2) keV and a mixing fraction of $(0.85 \pm 0.45)\%$ in the IBEC of ^{55}Fe, and Zlimen *et al.* [5] reported a $17.2^{+1.3}_{-1.1}$ keV mass component with a $(1.6 \pm 0.7)\%$ mixing in ^{71}Ge; experiments conducted by Borge *et al.* [12] failed to observe any anomaly in the IBEC spectra of ^{125}I. Norman has recently remeasured the decay of ^{55}Fe and found no evidence for a heavy neutrino [18].

The purpose of this paper is to present the results of an IBEC experiment on ^{71}Ge conducted at the TANDAR laboratory in Buenos Aires. A progress report of these results was presented in Ref. [19]. The aim of the experiment was to increase by at least an order of magnitude the statistics of the counted photons with respect to that of Ref. [5] in order to improve the sensitivity to the expected anomaly and shed light on the current discrepancy between the different IBEC results. To achieve this we had to pay special attention to the determination of the detector response function, the detector efficiency—including effects due to the finite size of the source and photon self-absorption—as well as the subtraction of the room background, pileup, and residual contaminants. The outline of the paper is as follows. In Sec. II we describe the experimental procedure. A description of the methods used and developed to reduce the data is given in Sec. III. The analysis of the data and the results are given in Sec. IV. Finally, the conclusions are presented in Sec. V.

II. EXPERIMENTAL PROCEDURE

The decay of ^{71}Ge ($T_{1/2} = 11.2$ d) occurs via an allowed transition to the ground state of the daughter nucleus and no γ rays are emitted. The ^{71}Ge source was obtained through an (n, γ) reaction on natural germanium. A disklike shape piece (diameter of 16 mm, thickness of 0.3 mm) of a high purity crystal of natural germanium was irradiated during 30 days with a neutron flux of approximately 2×10^{13} neutrons/cm^2 s, provided by the RA3 Ezeiza nuclear reactor, near Buenos Aires. A source of approximately 1 Ci was obtained at the end of the irradiation. We started our measurements about 40 days after the end of the irradiation to reduce the radioactive impurities of ^{77}Ge ($T_{1/2} = 11.3$ h), ^{77}As ($T_{1/2} = 38.8$ h), and ^{69}Ge ($T_{1/2} = 39.0$ h) to levels lower than 10^{-8} of the ^{71}Ge activity.

Gamma rays were detected in a 58-mm-diam 78-mm-length coaxial HPGe detector with an energy resolution [full width at half maximum (FWHM)] of 1.2 keV at 200 keV. The source was mounted at 1 cm in front of the detector. The source and the detector were shielded locally with aluminum, iron, and tantalum foils to reduce fluo-

rescence x rays, and the whole setup was surrounded by a shielding of lead bricks. Pulses from the detector were amplified and shaped by an ORTEC 673 amplifier operating with 6-μs shaping constants. In order to reduce the pileup the signals were vetoed with a gate obtained from the amplifier pileup rejection system. The resolving time of the fast-amplifier circuit which generates the logic-inhibit pulse is of 0.3 μs measured using a pulse generator and is, to a large extent, independent of the shaping-time constant. A PCA-II/AT-based acquisition system was used to collect data in 8192 channels with an energy gain of 0.13 keV/channel, and recorded in 24-h cycles on disk. Measurements of the ^{71}Ge source in cycles of about 96 h were alternated with measurements of the room background in cycles of about 24 h during several days. In total, we counted for 750 live-time h with the source and 120 live-time h for the background. A signal from a pulser was fed through the preamplifier at a rate of 1 Hz to monitor possible gain and offset shifts. A maximum drift of $\pm$ 2 channels was observed, and all of the ^{71}Ge spectra were summed together without applying any gain or offset corrections. The total spectrum thus obtained is shown in Fig. 1. The result of summing all of the room background spectra is also shown in the figure.

III. DATA REDUCTION

To search for a possible mass component of the emitted neutrino in IBEC the measured and the theoretical spectra must be compared. Before this comparison is made, the raw spectrum has to be consolidated by subtracting the room background, the residual contaminants, and the pileup contributions. The theoretical spectrum has to be corrected for the detector efficiency and then convoluted with the experimental response function. Let us discuss in detail each of these corrections.

A. Detector efficiency

The efficiency of the detector was determined using calibrated point sources of ^{133}Ba, ^{152}Eu, and ^{182}Ta, which have several γ rays in the energy region we studied. In order to minimize summing effects due to γ rays in coincidence from these sources, we measured the efficiency of the detector as follows: First, we determined the efficiency of the detector for a far-distance geometry (20 cm) using the above-mentioned calibrated point sources and parametrizing the efficiency ε as a function of photon energy using the analytical function

$$\varepsilon \propto E^a \exp(b\, E^c), \tag{3.1}$$

where E is the photon energy and a, b, and c are the parameters to be fitted to the data. Since we measured relative efficiencies (the data are known to an overall normalization), Eq. (3.1) is written as a proportionality. The data points of the relative efficiency as a function of photon energy are displayed in Fig. 2. The best fit (solid curve) was obtained for $a = -0.74 \pm 0.02$, $b = -(6.205 \pm 0.002) \times 10^8$, $c = -4.45 \pm 0.02$, when E was expressed in keV. Having determined the efficiency in far-distance geometry we transformed this result to close-distance geometry (same as used for the ^{71}Ge IBEC spectrum measurements) by measuring the transformation curve of the efficiency from far- to close-distance geometry [20] (Fig. 3). This curve has to be measured by coincidence-free sources, and for this purpose we used ^{57}Co, ^{203}Hg, ^{137}Cs, and ^{54}Mn.

Since the ^{71}Ge source used in the present measure-

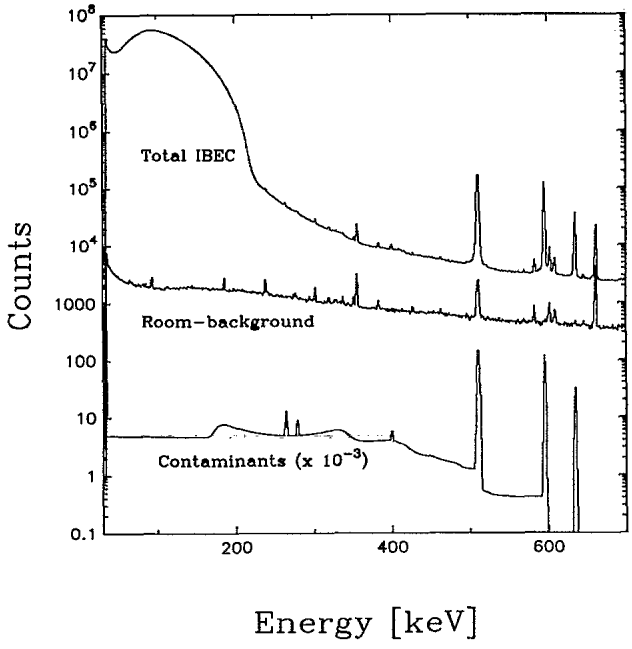

FIG. 1. Total experimental spectrum obtained with the ^{71}Ge source along with room background and residual contaminants spectra.

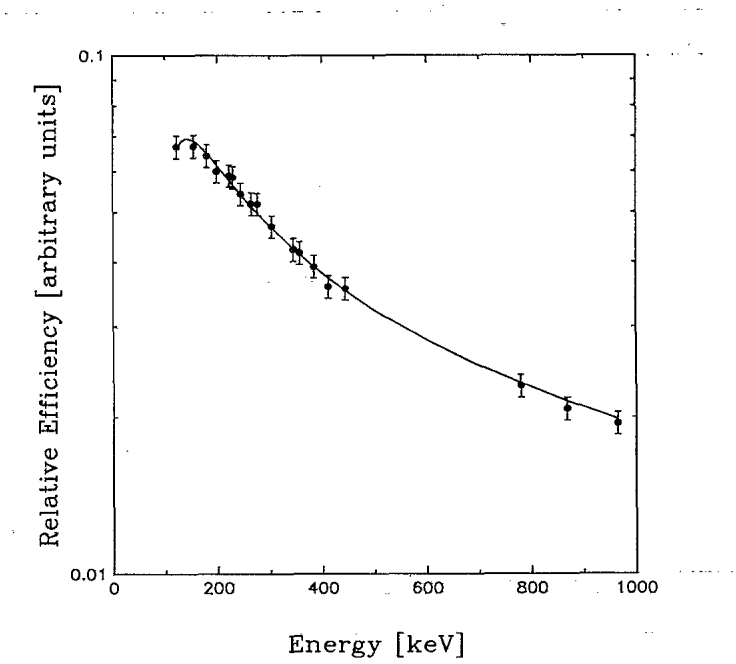

FIG. 2. Relative efficiency of the detector for a far-distance geometry as a function of photon energy.

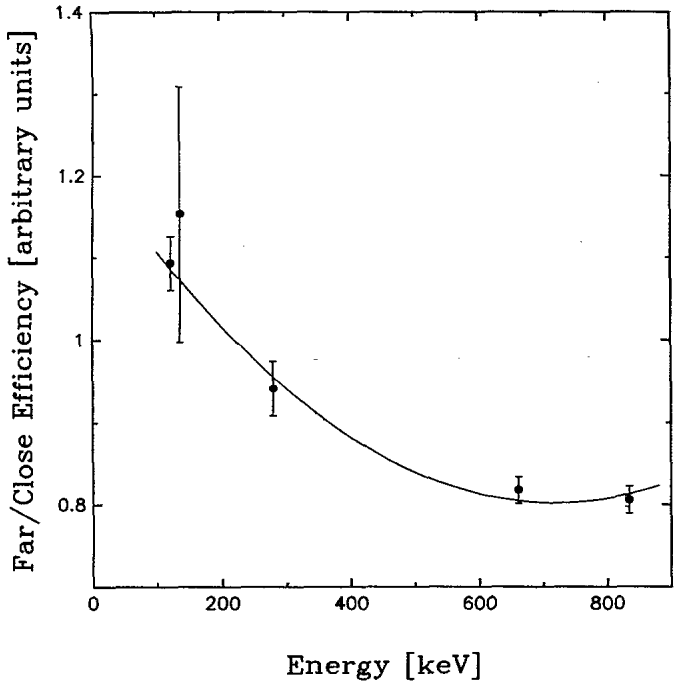

FIG. 3. Transformation curve of the detector efficiency from far- to close-distance geometry.

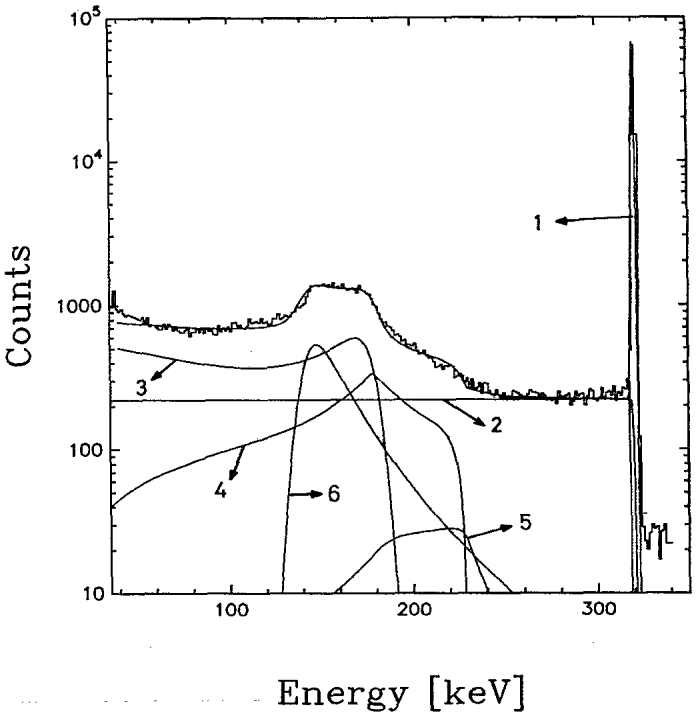

FIG. 4. Measured ^{51}Cr gamma-ray spectrum (histogram). The curves show the fitted total spectrum and its components labeled as (1) photopeak, (2) flat continuum, (3) single Compton scattering, (4) double Compton scattering, (5) triple Compton scattering, and (6) Compton backscattering.

ments consists of a piece of high purity crystal of natural germanium, we have investigated the effects of its finite size (disklike shape) and the effects of the photon absorption. The former was determined by measuring the difference in relative efficiency between two ^{182}Ta sources. One was a point source, and the other was one made of equal size and shape as the ^{71}Ge source. To correct for the self-absorption (as a function of the photon energy) the intensity of the IBEC spectrum generated by the ^{71}Ge source was measured relative to that obtained by placing a piece of a nonirradiated crystal of natural germanium with a thickness of 0.15 mm between the source and the detector. Both effects—finite size of the source and photon self-absorption—were parametrized as a function of photon energy with simple analytical functions and were included as corrections to the detector efficiency. The uncertainty in the energy dependence of the detector efficiency in the region of interest is less than 4%, taking into account all the effects discussed in this section.

B. Detector response function

The detector response function consists of a set of analytical functions describing the following features: photopeak, flat continuum, single, double, and triple Compton scattering, and Compton backscattering [21]. The parameters of the response function as a function of photopeak energy were determined using monoenergetic sources of ^{241}Am, ^{51}Cr, ^{198}Au, ^{137}Cs, and ^{54}Mn. As an example we show in Fig. 4 the best fit to the spectrum of ^{51}Cr including the different components of the response function. The comparison between the measured and the calculated single-line response function is excellent. The description of multiline sources such as ^{133}Ba is also very good. The response function was obtained with a twofold purpose: (a) to describe the spectrum of the residual contaminants used in the subtraction and (b) to convolute the theoretical spectrum in the fitting procedure. In the latter and given the width of the fitting intervals used in the analyses, the only two relevant parameters of the response function are the width of the Gaussian-shape photopeak and the magnitude of the flat continuum tail—the various Compton effects being excluded from the region of analysis.

C. Residual contaminants

Besides the room background there are two other sources of background: unrejected pileup pulses and residual contaminants. It can be seen from Fig. 1 that the only remaining residual contaminants present in the spectrum are ^{74}As ($T_{1/2}$ = 17.8 d) which decays emitting γ rays with energies of 511 keV, 595 keV, and 634 keV (part of the 511-keV contribution is also present in the room background) and ^{75}Se ($T_{1/2}$ = 119.8 d) with gamma energies of 264.7 keV, 279.5 keV, and 400.7 keV. The shapes of their corresponding photon spectra were modeled using the response function (including the summing effects for the 511- and 595-keV gamma rays), and were normalized to the photopeak areas of the total spectrum before the subtraction. Though *calculating* the contribution of the impurities may not be the best method to subtract them, the sensitivity of the final spectrum

to this subtraction was tested by changing the contribution of the full response with all its detail to that of a flat continuum without any structure (in the region of analysis), in particular that coming from the Compton backscattering. The conclusions from both analyses do not change in any appreciable way.

D. Pileup subtraction

Since we deal in this experiment with counting rates as high as 5000 counts per second, the accounting and subtraction of the pileup events merits special attention. The way this subtraction is usually carried out, as described in previous IBEC [5, 12] and β-decay [3, 4] experiments, turned out to be unsatisfactory in our case. Because of this, we developed a technique based on experimental observations. While it is clear that the contribution of the pileup to the measured spectrum becomes more important at higher counting rates, here we exploited the *observed fact* that the *shape* of the pileup spectrum does not depend on the counting rate (this latter affecting the intensity of the spectrum). The soundness of this assumption can be checked by looking at Fig. 5 where we show three spectra from which the room background and contamination contributions were subtracted, obtained at very different counting rates (from top to bottom 1500, 2800, and 4800 Hz) and all of them normalized in the region of pure pileup. With this hypothesis and once the background and contaminations are subtracted from the total spectrum, what remains is a spectrum with two components: *pure inner bremsstrahlung* and *pileup*.

Let us consider now two spectra obtained at different times, one at the beginning of the data taking when the counting rate was high (4800 Hz) and the other close to the end when the counting rate was low (1000 Hz). Clearly, the amount of pileup events present in the second spectrum is smaller than in the first one. If we normalize the inner bremsstrahlung component of both spectra and then perform a channel-by-channel subtraction, this component will cancel out and what remains will be the pileup contribution. We define $S(E)$ as the measured spectrum, $I_e(E)$ as the pure inner bremsstrahlung spectrum, and $P(E)$ as the pileup spectrum, such that

$$S_h(E) = \alpha_h\, I_e(E) + \beta_h\, P(E), \tag{3.2}$$

$$S_l(E) = \alpha_l\, I_e(E) + \beta_l\, P(E), \tag{3.3}$$

where labels h and l denote high and low counting rates, respectively. Since $S_h(E)$ is not proportional to $S_l(E)$, we obtain $P(E)$ from the difference,

$$\alpha_l S_h(E) - \alpha_h S_l(E) = (\alpha_l\beta_h - \alpha_h\beta_l)P(E). \tag{3.4}$$

For practical purposes we perform this normalization in a region where there is almost no pileup, namely, at the low-energy end of the measured spectrum ($E_1 \approx 40$ keV). The resulting spectrum will contain statistical fluctuations, and so a smoothing will be necessary to obtain the correct shape of $P(E)$. Having obtained $P(E)$, it is straightforward to get the pure inner-bremsstrahlung spectrum $I_e(E)$ by simple subtraction.

Two remarks on the procedure are in order.

(i) As mentioned above, we require a pileup free region to normalize both spectra; in practice, however, there is no region *absolutely free* of pileup events. In what follows we will examine the procedure in more detail to show that indeed the spectrum we obtain is $I_e(E)$. Let us call γ the normalization factor between $S_h(E)$ and $S_l(E)$; then the difference spectrum $S'(E)$ will be

$$\begin{aligned} S'(E) &= S_h(E) - \gamma S_l(E) \\ &= (\alpha_h - \gamma\alpha_l)I_e(E) + (\beta_h - \gamma\beta_l)P(E) \\ &\approx (\beta_h - \gamma\beta_l)P(E), \end{aligned} \tag{3.5}$$

since according to the prescription for normalizing $S_h(E)$ and $S_l(E)$, γ is given by

$$\gamma = S_h(E_1)/S_l(E_1) \approx \alpha_h/\alpha_l. \tag{3.6}$$

The total accumulated spectrum $S_T(E)$ obtained by adding all the measured spectra, to which we subtracted the background and contaminations as discussed before, can be written as

$$S_T(E) = \alpha_T I_e(E) + \beta_T P(E). \tag{3.7}$$

Since the normalization between S_T and S' in the region in which there is pure pileup ($E > Q$) can be carried out very accurately (at a level of $\pm 0.5\%$ obtained by inspecting the residual spectrum), the ratio λ between both spectra can be precisely determined, and used to obtain the final spectrum. Numerically, λ is given by

$$\lambda = \frac{\beta_T}{\beta_h - \gamma\beta_l}, \tag{3.8}$$

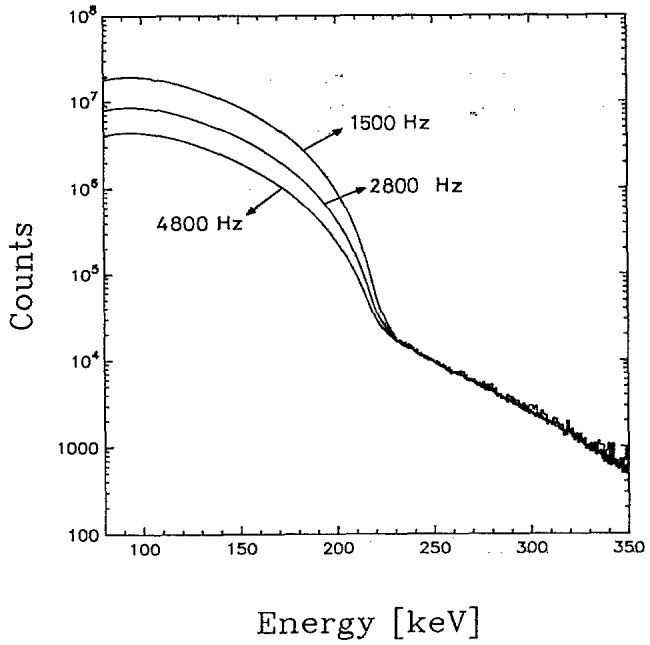

FIG. 5. Three pileup spectra obtained at different counting rates (from top to bottom 1500, 2800, and 4800 counts/s), normalized in the region of pure pileup, $E > Q_{EC} = 232.1$ keV.

whereas operationally λ was obtained by subtracting $\lambda S'(E)$ to $S_T(E)$ and requiring that the difference cancels out for $E > Q$. The final spectrum will be then

$$S(E) = S_T - \lambda S'(E), \tag{3.9}$$

which by using (3.5), (3.7), and (3.8) becomes

$$\begin{aligned} S(E) &= [\alpha_T - \lambda(\alpha_h - \gamma\alpha_l)]I_e(E) \\ &\quad +[\beta_T - \lambda(\beta_h - \gamma\beta_l)]P(E) \\ &= [\alpha_T - \lambda(\alpha_h - \gamma\alpha_l)]I_e(E). \end{aligned} \tag{3.10}$$

The term $\lambda(\alpha_h - \gamma\alpha_l)$ indicates whether the first normalization was correct. If done correctly, then $(\alpha_h - \gamma\alpha_l) = 0$ and this term vanishes. It is nonetheless remarkable that the spectrum $S(E)$ obtained through this procedure is, in any case, proportional to $I_e(E)$.

(ii) It could be argued that the procedure is not enough to obtain the proper pileup spectrum since, considering that events corresponding to a given channel ended up in another, the inner-bremsstrahlung spectrum will be distorted and the hypotheses used in writing down Eqs. (3.2) and (3.3) will be wrong. This, however, is not the case since the amount of counts lost from every channel is proportional to the intensity of the inner-bremsstrahlung spectrum in that particular channel. This conclusion can be arrived at in the following way. Given that the pileup spectrum is proportional to

$$\int_0^E I_e(x)\, I_e(E-x)\, dx, \tag{3.11}$$

the amount of events from a given channel (E_0) lost to the pileup spectrum is proportional to

$$I_e(E_0) \int_0^Q I_e(E)\, dE, \tag{3.12}$$

meaning that the events that are lost are proportional to $I_e(E_0)$ and therefore, after channel-by-channel subtracting $P(E)$ from the measured spectrum, the result will be the sought spectrum $I_e(E)$. Figure 6 shows the total experimental ^{71}Ge spectrum from which background and contaminants spectra have been subtracted, along with the resulting pileup spectrum.

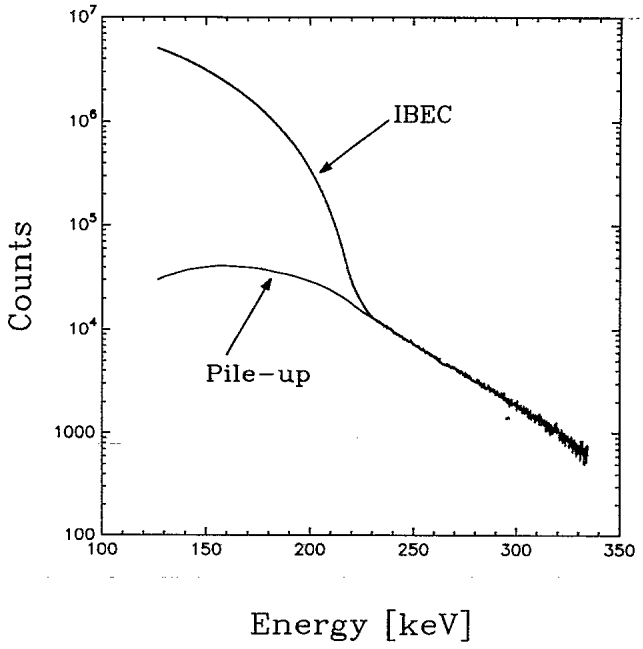

FIG. 6. Total experimental ^{71}Ge spectrum, from which room background and contaminants contributions have been subtracted, along with the resulting pileup spectrum.

IV. ANALYSIS OF THE DATA AND RESULTS

After subtracting the contributions, of room background, residual contaminants and pileup from the total spectrum, the experimental data were, thus, prepared for the fitting procedure. For the analysis we used the assumption of two neutrino mass eigenstates with the largest component (m_1) having zero mass. The capture rate as a function of photon energy E is given by

$$\frac{dW(E)}{dE} = \frac{dW(E, m_1 = 0)}{dE} \cos^2\theta + \frac{dW(E, m_2)}{dE} \sin^2\theta, \tag{4.1}$$

where the fraction of massive neutrinos is $\sin^2\theta$, and each term in Eq.(4.1) is of the form

$$\frac{dW(E, m_i)}{dE} = \sum_n \left[\frac{dW_{ns}(E, m_i)}{dE} + \sum_j \frac{dW_{np_j}(E, m_i)}{dE} + \cdots \right], \tag{4.2}$$

with n running over all the electronic shells. The theoretical IBEC rates for each shell were calculated using the method of Intemann [22] (for a review see Bambynek *et al.* [23]), and we allowed for the inclusion of electrons captured from the $1s$, $2s$, $2p$, and $3s$ shells. The rates are given by

$$\begin{aligned} \frac{dW_{ns}(E)}{dE} &\sim E\,[Q_{\rm EC} - B(ns) - E] \\ &\quad \times \left\{[Q_{\rm EC} - B(ns) - E]^2 - m_2^2c^4\right\}^{1/2} R_{ns}(E) \end{aligned} \tag{4.3}$$

for s states and,

$$\begin{aligned} \frac{dW_{np_j}(E)}{dE} &\sim E\,[Q_{\rm EC} - B(np_j) - E] \\ &\quad \times \left[(Q_{\rm EC} - B(np_j) - E)^2 - m_2^2c^4\right]^{1/2} \\ &\quad \times Q^2_{np_j}(E) \end{aligned} \tag{4.4}$$

for capture from p states. In the above $Q_{\rm EC}$ is the energy of the transition and $B(ns)$ and $B(np_j)$ are the binding energies of the s- and p-shell electrons, respectively. The R_{ns} and Q_{np_j} functions correct for Coulomb and relativistic effects. The theoretical spectrum was corrected to take into account the detector efficiency and the self-absorption and finite size of the source. The resulting

spectrum was finally convoluted with the experimental detector response function.

The analysis was done as follows. On the assumption of two neutrino masses present in the experiment with the lightest one kept fixed ($m_1 = 0$), we have three parameters to fit in the theoretical spectrum: the electron-capture Q value ($Q_{\rm EC}$), the heavy neutrino mass (m_2), and the mixing fraction ($\sin^2\theta$). It is known [23] that the theory reproduces the spectral shape of the contributions from the different shells much more accurately than their absolute magnitudes since there exists ambiguities between the experimental and calculated electron-capture ratios (i.e., the observed P_L/P_K, defined as the ratio of capture probabilities, is different from the predicted L/K capture ratio). Therefore, we weighted with a parameter A, the ratio between the first two major shells —K ($1s$) and L ($2s$ and $2p$)—in addition to considering an overall normalization constant (C). An energy-dependent shape factor $[P(E) = 1 + \beta(Q_{\rm EC} - E)]$ was included to compensate for small uncertainties in the determination of the detector efficiency ($\leq 4\%$) and to absorb possible deviations—very difficult to assess—in the shape of the pileup spectrum into the region of interest. Thus, for the fitting procedure we used a total of six parameters: $Q_{\rm EC}$, m_2, $\sin^2\theta$, C, A, and β.

The background-subtracted experimental spectrum was analyzed in an energy interval ranging from 180 to 220 keV and compressed into 0.5-keV-wide bins (81 data points). A least-squares fit of the experimental data was performed by comparing the theoretically expected spectrum for given values of m_2 and $\sin^2\theta$, and allowing the other four parameters to vary simultaneously. The contour plot of χ^2 as a function of the neutrino mass and the mixing fraction is shown in Fig. 7. The value of χ^2 obtained under the assumption of a single massless neutrino was 83.8. The minimum value of χ^2 was 82.6 and is indicated by a *star* in Fig. 7. The difference in χ^2 between this minimum and the value obtained under the assumption of single massless neutrino ($\Delta\chi^2 = 1.2$) has no statistical significance. Moreover, the 90% confidence level contour, which lies at approximately $\chi^2 = 87.2$ (4.6 units higher than the absolute minimum), is open and includes zero. The result of Ref. [5], namely a $17.2^{+1.3}_{-1.1}$ keV neutrino with $\sin^2\theta = (1.6 \pm 0.7)\%$, is also indicated in the figure with the label A. The massive neutrino defined at the lower ends of m_2 and $\sin^2\theta$ corresponds to a χ^2 of 92. This means that it can be excluded at a confidence level of 99.0% ($\Delta\chi^2 = 9.4$). It is interesting and curious to note that Borge *et al.* also found a local minimum at the same mass value corresponding to our best fit but at a very different mixing fraction, with similar lack of statistical significance (see Fig. 3 of Ref. [12]). Further analyses carried out using data compressed in 1-keV-wide bins and/or in the energy range of 150–220 keV yield similar results.

The values obtained for the parameters at the minimum of χ^2, quoted with 1σ statistical uncertainty, are the following: $\beta = (2.2 \pm 0.7) \times 10^{-4}$ keV^{-1}, $A = 1.04 \pm 0.05$, and $Q_{\rm EC} = 232.1 \pm 0.1$ keV. The small value of the parameter β indicates a weak energy dependence of the shape factor. The slight 4% deviation in the value of the parameter A with respect to that given by Intemann [22] is within the existing uncertainty bounds between theoretical and experimental values for P_L/P_K ratios as given in Table XV of Ref. [23]. We found that it is important to include the contribution of the $3s$ subshell (which does it at a level of about 1% with respect to the K shell) and also to allow for some latitude in the L/K ratio through the parameter A. This approach has made the local minimum reported in a preliminary analysis of this experiment [19] statistically much less significant. The $Q_{\rm EC}$ value is in agreement with the 231 ± 3 keV obtained by Bisi *et al.* [24], but differs from the 235.7 ± 1.8 keV of Wapstra and Audi [25] and the $229^{+1.1}_{-0.9}$ keV reported in Ref. [5].

We performed a series of tests to establish the sensi-

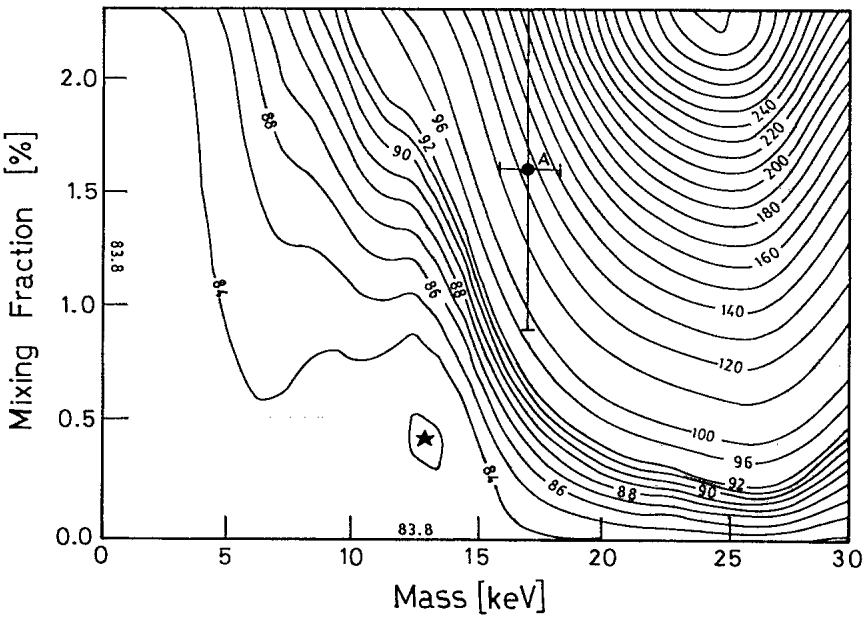

FIG. 7. Contour plot of χ^2 as a function of the neutrino mass and the mixing fraction. The absolute minimum is indicated by a *star*. The data point $m_2 = 17.2^{+1.3}_{-1.1}$ keV (95% C.L.) and $\sin^2\theta = (1.6 \pm 0.7)\%$ (95% C.L.) corresponds to the result of Ref. [5] (A).

tivity of our results to the uncertainties in the efficiency and response function of the detector, and in the subtraction of the pileup and background spectra. Special attention was paid to the systematic errors introduced by the subtraction of the pileup spectrum which was obtained using our unconventional method. The latter were estimated to be less than 5% in $\sin^2\theta$ and were negligible in m_2 and $Q_{\rm EC}$. From these analyses and by summing in quadratures the different sources of error, including the uncertainty of the energy calibration (≤ 0.2 keV), we determined the systematic errors in m_2, $\sin^2\theta$, and $Q_{\rm EC}$ to be 2%, 10%, and 0.1%, respectively. For the parameter β the systematic error is negligible, whereas A receives a contribution of 6%.

Figure 8 shows the ratio of the data (compressed to 0.5 keV/channel) to the theoretical fit assuming the emission of a single massless neutrino. For this least-squares fit the parameters $Q_{\rm EC}$, C, A, and β were allowed to vary simultaneously. The horizontal line represents the shape expected for zero-mass neutrinos. The solid curve corresponds to the ratio of the theoretical prediction obtained with $m_2 = 17$ keV and a mixing fraction $\sin^2\theta = 1.0\%$ to that obtained with $m_2 = 0$. We set an upper limit of 0.5% mixing fraction for a 17-keV neutrino at 95% confidence level. In Fig. 7 this confidence level contour corresponds to a χ^2 of 88 which for a 17-keV neutrino gives a mixing fraction of 0.45%. Taking into account systematic errors of about 10% in $\sin^2\theta$, an upper limit of 0.5% was thus obtained.

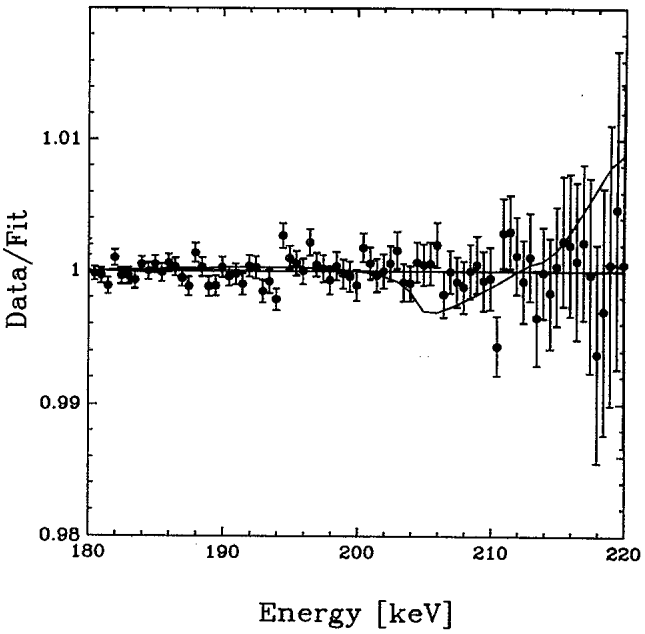

FIG. 8. Experimental data normalized to the best theoretical fit with a single massless neutrino. The solid line corresponds to the ratio of the theoretical prediction obtained with $m_2 = 17.0$ keV and a mixing fraction $\sin^2\theta = 1.0\%$ normalized to that obtained with $m_2 = 0$.

V. CONCLUSIONS

To conclude, we have measured the internal bremsstrahlung spectrum of the electron capture (IBEC) decay of ^{71}Ge in search for a possible mass component of the emitted neutrino. The present experiment has 20 times more statistics than a previously reported work [5] for the decay of the same nucleus, thus improving the sensitivity to the expected anomaly in the spectrum. Special attention was paid to the determination of the detector response function, the detector efficiency, including effects due to the finite size of the source and photon self-absorption, as well as the subtraction of the room background, pileup, and residual contaminants. The analysis of the experimental data shows no indication of the $17.2^{+1.3}_{-1.1}$ keV neutrino with a mixing fraction of $(1.6 \pm 0.7)\%$, as claimed by the Zagreb group [5], at a 99.0% confidence level.

ACKNOWLEDGMENTS

The authors would like to thank the personnel at the Ezeiza RA3 reactor for their assistance in the preparation of the source, and to A.O. Macchiavelli for carefully reading the manuscript and for his helpful comments. Financial support from the Fundación ANTORCHAS is gratefully acknowledged. D.E.D.G. and A.O.G. acknowledge the financial support of the Consejo Nacional de Investigaciones Científicas y Técnicas, Argentina.

[1] A compendium of the experimental and theoretical activity related to the 17-keV neutrino (by early 1992) can be found in Proceedings of the Workshop on the 17-keV Neutrino Question, Center for Particle Astrophysics, Berkeley, California, 1991 (unpublished).
[2] E.B. Norman, B. Sur, K.T. Lesko, M.M. Hindi, R.M. Larimer, T.R. Ho, J.T. Wiltort, P.N. Luke, W.L. Hansen, and E.E. Haller, in Proceedings of the Fourteenth Europhysics Conference in Nuclear Physics, Bratislava, Czechoslovakia, 1990 (to be published).
[3] A. Hime and N. Jelley, Phys. Lett. B **257**, 441 (1991).
[4] A. Hime, Ph.D. thesis, Oxford, 1991; Oxford Report No. OUNP-91-20, 1991.
[5] I. Zlimen, A. Ljubicic, S. Kaucic, and B.A. Logan, Phys. Rev. Lett. **67**, 560 (1991).
[6] J.J. Simpson and A. Hime, Phys. Rev. D **39**, 1825 (1989); **39**, 1837 (1989).
[7] B. Sur, E.B. Norman, K.T. Lesko, M.M. Hindi, R.M. Larimer, P.N. Luke, W.L. Hansen, and E.E. Haller, Phys. Rev. Lett. **66**, 2444 (1991).
[8] T. Altzitzoglou, F. Calaprice, M. Dewey, M. Lowry, L. Piilonen, J. Brorson, S. Hagen, and F. Loeser, Phys. Rev. Lett. **55**, 799 (1985).
[9] T. Ohi, M. Nakajima, H. Tamura, T. Matsuzaki, T. Yamazaki, O. Hashimoto, and R.S. Hayano, Phys. Lett. **160B**, 322 (1985).
[10] J. Markey and F. Boehm, Phys. Rev. C **32**, 2215 (1985).
[11] D.W. Hetherington, R.L. Graham, M.A. Lone, J.S.

Geiger, and G.E. Lee-Whiting, Phys. Rev. C **36**, 1504 (1987).
[12] M.J.G. Borge, A. de Rujula, P.G. Hansen, B. Jonson, G. Nyman, H.L. Ravn, and K. Riisager, Phys. Scr. **34**, 591 (1986).
[13] I. Zlimen, S. Kaucic, A. Ljibicic, and B.A. Logon, Phys. Scr. **38**, 539 (1988).
[14] J.J. Simpson, Phys. Rev. Lett. **54**, 1891 (1985).
[15] H. Kawakami, S. Kato, T. Ohshima, C. Rosenfeld, H. Sakamoto, T. Sato, S. Shibata, J. Shirai, Y. Sugaya, T. Susuki, K. Takahashi, T. Tsukamoto, K. Ueno, K. Ukai, S. Wilson, and Y. Yonozawa, Phys. Lett. B **287**, 45 (1992).
[16] J.L. Mortara *et al.*, Phys. Rev. Lett. **70**, 394 (1993).
[17] A. Hime, LANL Report No. LA-UR-92-3087, 1992.
[18] E.B. Norman (private communication).
[19] D.E. DiGregorio, S. Gil, H. Huck, E.R. Batista, A.M.J. Ferrero, and A.O. Gattone, in Proceedings of the Workshop on the 17-keV Neutrino Question, Center for Particle Astrophysics, Berkeley, California, 1991 (unpublished), p. 347.
[20] S. Gmuca and I. Ribansky, Nucl. Instrum. Methods A **202**, 435 (1982).
[21] M. C. Lee, K. Verghese, and R.P. Gardner, Nucl. Instrum. Methods A **262**, 430 (1987).
[22] R.L. Intemann, Phys. Rev. C **3**, 1 (1971).
[23] W. Bambynek, H. Behrens, M.H. Chen, B. Crasemann, M.L. Fitzpatrick, K.W.D. Ledingham, H. Genz, M. Mutterer, and R.L. Intemann, Rev. Mod. Phys. **49**, 1 (1977).
[24] A. Bisi, E. Germagnoli, L. Zappa, and E. Zimmer, Nuovo Cimento **2**, 290 (1955).
[25] A.H. Wapstra and G. Audi, Nucl. Phys. **A432**, 1 (1985).